GMGDA 2019

Floor damage mechanism with cemented paste backfill mining method

Xianyuan Shi [1,2,3] · Huaqiang Zhou [1] · Xikui Sun [2] · Zhong Cao [2] · Qingmin Zhao [2]

Abstract

This paper aims to address the coal seam floor behavior after mining with CPB method. Firstly, the numerical model by using Midas/GTS-Flac[3d] method is developed on the basis of 2353 working face, Daizhuang Coal Mine; then, the slip line field theory of plastic mechanics is applied to calculate the floor damage depth. Furthermore, field observation is carried out by using water injection method. The results show that the floor deformation is well controlled by using CPB; the tensile zone reduces greatly to one-sixth of the size with traditional caving mining method; the coal seam excavation with CPB mining method is equivalent to reducing the original mining thickness; and the depth of the fracture floor is around $2 \sim 4$ m. The numerical simulation and analytical calculation in terms of floor damage depth coincide with the in situ measurement. The proposed analytic model provides insight into the floor behavior with backfilling mining method.

Keywords CPB · Floor failure · Confined aquifer · Field measurement

Introduction

Cemented paste backfill (CPB) is widely used in mining engineering for its environmentally friendly and support capacities. Coal mining involves the creation of voids, which induces the instability of the surrounding rocks. The backfilling with CPB enables stabilizing local stresses, minimizes the roof and floor closure, and reduces the environmental pollution. However, the mining regions in North and South China often encounter water inrush risks, and the understanding of using CPB is important to maintain the safety mining operation in such conditions.

This article is part of the Topical Collection on *Geological Modeling and Geospatial Data Analysis*

✉ Xianyuan Shi
  sxy296@163.com

1 Key Laboratory of Deep Coal Resource Mining, Ministry of Education of China, China University of Mining and Technology, Xuzhou 221116, China

2 Shandong Energy Zibo Mining Group Co., Ltd., Zibo 255000, China

3 Shandong Kang Ge Energy Technology Co., Ltd., Jining 272000, China

In recent decades, the investigations on water inrush mechanisms have been highlighted. The underground excavation-induced stability issue attracts increasing interest (Chen 2013; Zhang and TianQuan 1990; Dong et al. 2018a; Dong et al. 2019a, b; Dong et al. 2018b). The stress and deformation change accordingly with the excavation process. A number of empirical criteria and analytical models have been proposed for the analysis and predication of water inrushes from underlying confined aquifers, including the water inrush index, hypothesis of three zones in floor strata, plate model, and key strata model (Zhang and Huang 2019; Zhang et al. 2016; Wang and Park 2003; Lai et al. 2006; Zhang 2005; Lu and Wang 2015; Zhu and Wei 2011; Yin et al. 2016).

Since 2010, more than 84 water inrush tragedies happened during underground mining excavations in China, including 9 non-coal mine accidents, causing 455 deaths (State Administration of work safety 2017). Mine water damage control is a key to maintain highly efficient and safety excavations. The confined aquifer of the floor strata is the most serious type of mine water damage. Quan et al. (Xiucai et al. 2016) applied the elastic thin plate theory to analyze the mining-induced failure mechanism of the floor under confined aquifer. Yao et al. (Duoxi and Lu 2010) used Flac3D to study the fluid-solid coupling of the deformation and failure law of coal mining floor under confined aquifer condition. Different factors influencing the depth of the damaged floor were

investigated in detail. Jiang et al. (Yaodong et al. 2011) conducted similar simulation experiments to investigate the evolution of the stress field and displacement field of the floor of the working face of the Kowloon Mine under confined aquifer. Zhang et al. (Fengda et al. 2016) combined fracture mechanics and unified strength theory to reveal the mechanism of water inrush failure under the unloading action. Zhang et al. (Songping et al. 2006) used the seismic CT detection technology to measure the depth of the floor failure. Sun Jian et al. (Jian et al. 2011) used microseismic technology to dynamically monitor the failure characteristics of the inclined coal seam floor in the mining water conservancy of Taoyuan Mine. Duan et al. (Hongfei et al. 2011) and Zhang et al. (Rui et al. 2012) used the strain monitoring system to study the damage law of thick coal seam and thin coal seam floor, respectively. Shi et al. (Qinglong et al. 2013) used the Matlab software to fit the nonlinear regression formula of the damage depth of the floor strata based on a large number of measured data. Wang et al. (Wang et al. 2013) further calculated the stress of the floor of the stope based on the mine pressure and key layer theory. In addition, Yu et al. (Yu et al. 2009) and Zhang et al. (Wenquan et al. 2015) used BP neural network and gray correlation theory to predict the damage depth of the floor strata, respectively.

Many case studies show that the failure character of the coal seam floor is not only related to basic geological condition such as rock properties, ground stress, and working face size, but also affected by the treatment method of empty space. The damage law of floor under CPB effect is obviously different from the traditional caving method (Qingliang et al. 2016). Based on the engineering background of the 2353 paste working face of Daizhuang Coal Mine, this paper studies the CPB effect on the failure law of the floor. The failure law of the coal floor is investigated by Flac3D modeling, and the actual damage depth of the bottom plate is detected by in situ measurement. The research can improve the reference for guiding the safe mining under confined aquifer condition.

Geological conditions

Daizhuang Coal Mine was completed and put into operation in 2000 with an annual production capacity of 3 million tonnes operated by Zibo Mining Group. The main mineable coal seams are 3#, 16#, and 17#. The studied backfilling working face with cemented paste backfill (CPB) is 2353 working face, which belongs to 3# coal seam. The buried depth of the coal seam is 430 m. The strike length of the mining area is 730 m, and the working face is 150 m long. The coal seam has an average thickness of 2.70 m and a dip angle of 4°.

Based on the drilling data of the working face, the immediate roof of the 3# coal seam is mudstone and sand mudstone,

which belongs to the layer type and is a medium stable roof. The coal seam floor is siltstone and fine sandstone. The main threat of the mining area is the Ordovician limestone and other huge thick karst-confined water under the coal seam floor, and the measured water pressure was 4.38 MPa in 2013. In addition to assess the confined aquifer risk through detailed investigation of the mining area, the CPB technology is applied during the production to minimize the mining disturbance on the floor. In this application, the mass concentration of CPB is 74%, and the mass ratio of cement, fly ash, and coal gangue is 1:4:6. The backfilling capacity reaches 170 m^3/h.

CPB mining mechanism on the floor damage

Floor damage depth with equivalent mining height

The floor damage mechanism and characteristics with CPB backfilling mining technology are different from those of caving mining method. This leads to different disturbance depth of the surrounding rocks between these methods. When the backfilling mining method is used, the coal seam excavation is equivalent to reducing the original mining thickness. In the literature, many researchers have established a plenty of empirical formulas that provided the relationship between the equivalent mining height with backfilling and the traditional caving method. Guo et al. (Guo et al. 2014) found that the equivalent mining height is only a few hundred millimeters for 2.5-m thickness coal seam.

There are many factors influencing the water inrush from coal seam floor such as the water-rich aquifer, water pressure, and water-bearing rock formation. Among them, the water-rich aquifer and water pressure are invariable. When the working face advances, the integrity of the coal seam floor is destroyed under the excavation disturbance. The thickness of the water-bearing rock formation is, therefore, reduced. The previous numerical simulation results in Fig. 1 with caving mining method showed that in the range of small mining
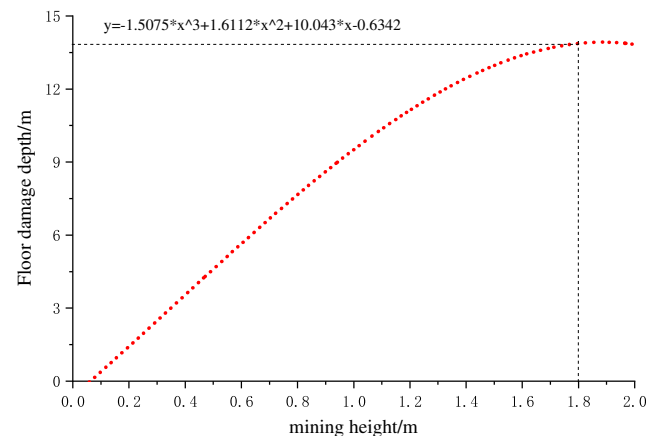

Fig. 1 Relationship between mining height and floor damage depth

height (0 ~ 1.8 m), the floor damage depth is highly dependent on the mining height. However, when the mining height reached a certain level (> 1.8 m), the floor damage depth shows an independent tendency with the mining height.

CPB induced failure characteristics of the floor

The numerical simulation model is constructed to investigate the failure evolution process of the coal seam floor under CPB mining. The general-purpose commercial software Flac^{3d} is used for this simulation. The model size is 400 m × 150 m × 130 m (see Fig. 2). The side boundaries are restricted to move in horizontal directions, and the bottom of the model is fixed. In order to reduce the model boundary effect, a free boundary of 50 m is left on both sides of the model. Different mesh sizes were set for different rock formations in Midas/GTS and then imported into Flac^{3d} for post-processing analysis. Local fine mesh is used near the coal seam. The equivalent load of 300 × 2500 × 10 = 7.5 MPa is applied to the upper boundary of the overlying missing strata.

The mechanical parameters of the simulation are obtained through the on-site coal rock sampling and indoor rock mechanics tests (see Table 1). The mechanical properties of the CPB are measured by using the light geological drilling in the mining field on the 2353 working face along the roadway to drill the core of the CPB, which has 28-day age strength.

The complex in situ geo-stresses are considered in this simulation. According to the statistics in the literature(Weidong et al. 2015), the horizontal and vertical stress expressions are summarized in Eq. (1):

$$\begin{cases} \sigma_z = 0.0276H\text{-}1.6487 \\ \sigma_H = 0.0413H\text{-}1.7725 \\ \sigma_h = 0.0324H\text{-}7.6975 \end{cases} \quad (1)$$

where σ_z, σ_H, and σ_h represent the vertical, maximum horizontal, and minimum horizontal stresses, respectively in MPa, and H is the buried depth, m.

Figure 3 shows the plastic zone development due to CPB mining. Either the tension or shear stress exceeds the strength threshold of the floor which would cause floor failure. The floor damage depth is qualitatively determined based on the range of the plastic zone. With the advances of the working face, the plastic zone extends gradually into the floor and eventually reaches a stable value (Fig. 3b and c). When the working face is filled for 200 m, the size of the plastic zone has not expanded, and the final saddle-shaped plastic zone also confirms the stable of plastic zone. The maximum failure depth of the coal seam floor reaches 3 m. It can be seen that the failure characteristic of the coal seam floor stratum first enters the shear plastic yielding status, and then the type changes to tensile yielding damage. It is noted that the simulation results can only qualitatively indicate the floor damage depth, given the complex geological condition of the original problem and the coarse mesh of the model.

The field observation results show that with the advancement of the working face, the coal seam floor is compressed under the supporting pressure. After the working surface is advanced, the stress is released, and the bottom plate is in an expanded state. With the fall of the roof rock stratum and the compaction of the falling rock in the goaf, the coal seam floor is restored to the original stress state.
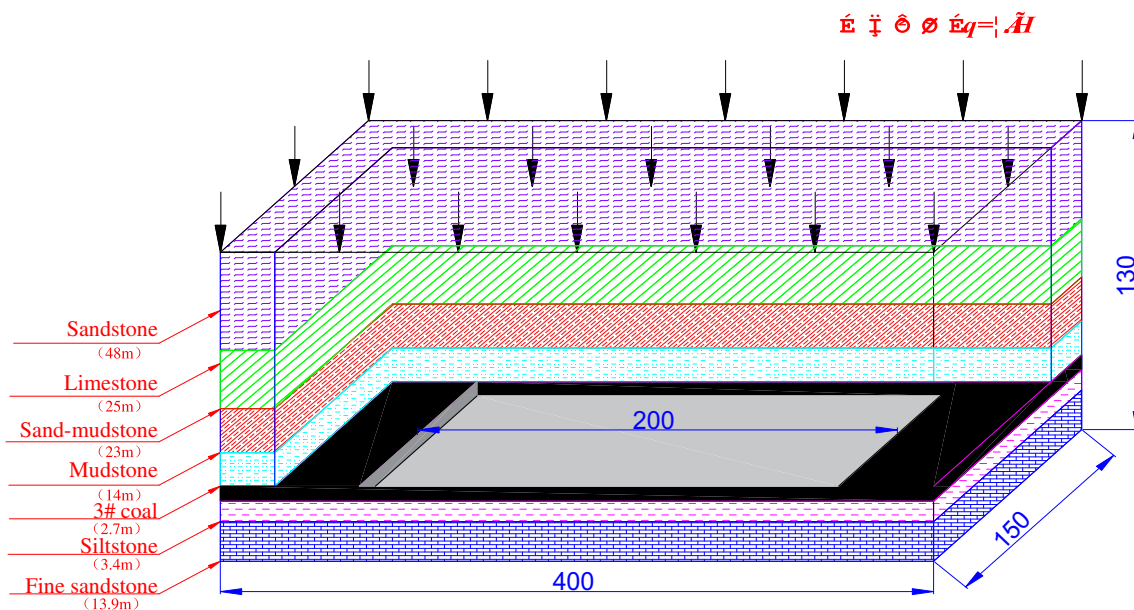

Fig. 2 Model of overall geometry

Table 1   Mechanical parameters of rock mass

Strata	Thickness/m	Density/kg·m^{-3}	Bulk modulus/GPa	Shear modulus/GPa	Internal friction angle/°	Cohesion/MPa	Tensile strength/MPa
Sandstone	48	2580	12.22	10.79	42	2.5	3.6
Limestone	25	2800	5.57	4.53	38	11.4	6.7
Sand mudstone	23	2520	4.9	3.2	35	1.18	1.8
Mudstone	14	2891	2.17	1	39.4	1.3	1.15
3# coal	2.7	1400	2.08	0.54	25	0.5	0.64
Siltstone	3.40	2630	5	3.8	35	6	2.5
Fine sandstone	13.9	2721	3.47	2.08	37.6	5.2	2.81
CPB	–	2000	2	2	15	0.3	0.70

The stress variation of the floor is shown in Fig. 4. With the advancement of CPB mining, when the propulsion is 50 m, the roof of the coal seam is not broken, which acts as a composite beam. The load on the CPB is small, and less than 2.5 MPa. When the excavation exceeds 100 m, the CPB tends to be stable, and the final vertical stress is 5 MPa, which is 0.5 times of the original stress field. It can be seen that the CPB plays the role of pressure relief and control of surrounding rock movement and deformation.

(a)

(b)

(c)

(d)
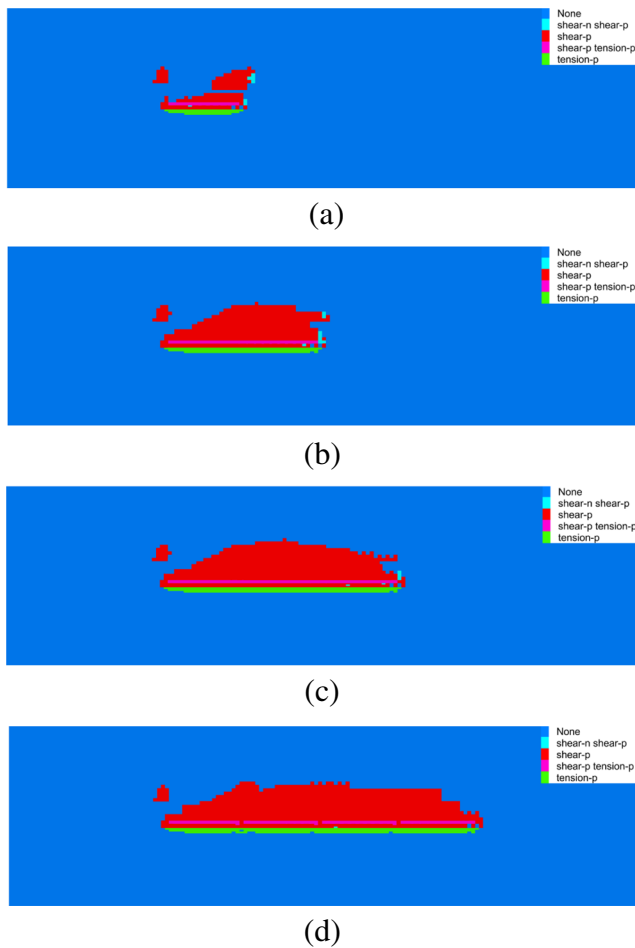
Fig. 3 Plastic zone development with CPB mining method. **a** Advancing 50 m. **b** Advancing 100 m. **c** Advancing 150 m. **d** Advancing 200 m

(a)

(b)

(c)

(d)
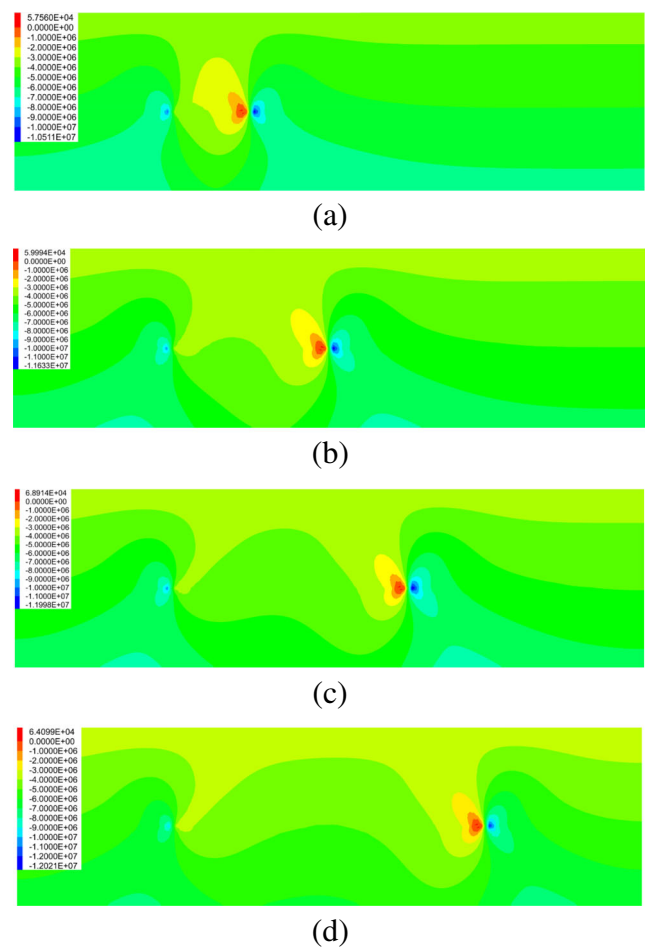
Fig. 4 Vertical stress contour. **a** Advancing 50 m. **b** Advancing 100 m. **c** Advancing 150 m. **d** Advancing 200 m

Theoretical analysis of the floor damage zone

Maximum floor damage depth

It is known that the progress of the abutment pressure due to mining is the cause of the floor stratum damage, including the compression and the bulking phenomena. When the abutment pressure on the coal seam floor reaches the strength threshold, a plastic zone is formed within a certain range below the coal seam. The analytical model is shown in Fig. 5. The abutment pressure increases in both coal seam and floor. We adopted the slip line field theory of plastic mechanics, and the disturbed floor is divided into three zones, namely active limit zone (Fig. 5I), transition zone (Fig. 5II), and passive limit zone (Fig. 5III).

The movement is deformed to form a continuous slip surface. As shown in Fig. 5, the active limit zone (I) consists of an isosceles triangle shape $ab\,a'$ ($ab = a'\,b$). The points a and a' represent the position of the working face and the peak abutment pressure on the coal seam, respectively. The distance between the working face and the peak abutment pressure is detonated as $aa' = x_a$ (plastic zone width). The angle between the coal seam floor and the triangle edge $a'\,b$ is $45^\circ + \varphi_0/2$. The abutment pressure in active limit zone is transmitted into the passive zone through transition zone (II), which covered under the logarithmic helix curve BEC with an expression of

$$r = r_0 e^{\theta \tan \varphi_0} \tag{2}$$

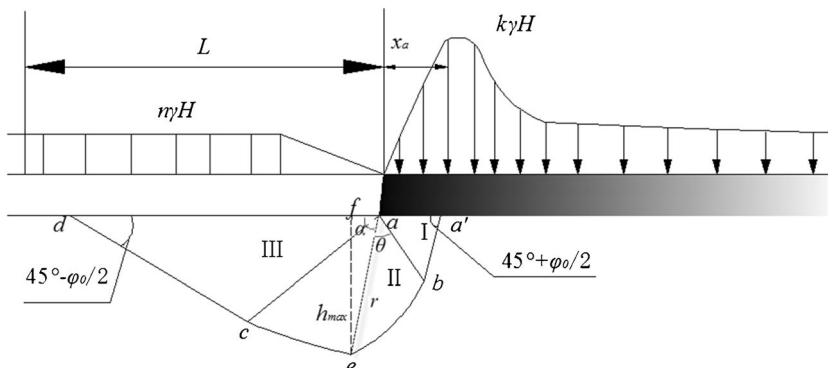where r_0 represents the length of ab and can be expressed as

$$r_0 = x_a / 2\cos\left(\frac{\pi}{4} + \frac{\varphi_0}{2}\right) \tag{3}$$

The maximum damage depth is observed in this zone. The angle between triangle edge cd in the passive zone (III) and coal seam is $45^\circ - \varphi_0/2$ (see Fig. 5). Based on the geometry relationship, we have

$$h = r\sin\alpha \tag{4}$$

where $\alpha = \frac{\pi}{2} - \left(\theta + \frac{\varphi_0}{2} - \frac{\pi}{4}\right)$.

Substituting Eqs. (2) and (3) into Eq. (4), the damage depth has the following form:

$$h = r_0 e^{\theta \tan \varphi_0} \cos\left(\theta + \frac{\varphi_0}{2} - \frac{\pi}{4}\right) \tag{5}$$

The maximum depth is obtained when the condition $\frac{dh}{d\theta} = 0$ is met:

$$r_0 e^{\theta \tan \varphi_0} \cos\left(\theta + \frac{\varphi_0}{2} - \frac{\pi}{4}\right)\tan\varphi_0 - r_0 e^{\theta \tan \varphi_0}\sin\left(\theta + \frac{\varphi_0}{2} - \frac{\pi}{4}\right)$$
$$= 0 \tag{6}$$

The θ is obtained:

$$\theta = \frac{\varphi_0}{2} + \frac{\pi}{4} \tag{7}$$

Therefore, the expression of the maximum damage depth is given as

$$h_{\max} = \frac{x_a \cos\varphi_0}{2\cos\left(\frac{\pi}{4} + \frac{\varphi_0}{2}\right)} e^{\left(\frac{\pi}{4} + \frac{\varphi_0}{2}\right)\tan\varphi_0} \tag{8}$$

Determination of the plastic zone width

Apart from the field measurement in determining the plastic zone width, the theoretical analysis can be an alternative way. The limit equilibrium theory is used assuming that the coal seam is stable under the current stress status as shown in Fig. 6.
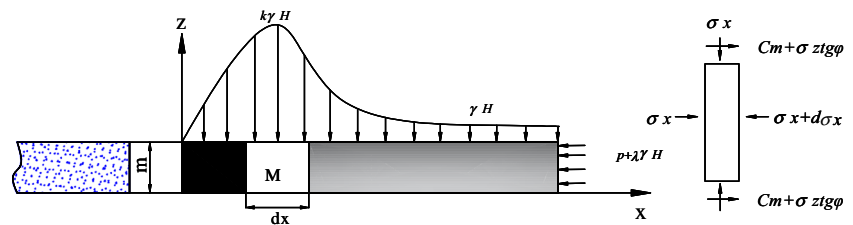
An arbitrary element unit (M) in the coal seam is selected with a width of dx. The zero-resultant force in the x-axis direction is written as

$$2C_m + 2\sigma_z \tan\varphi - \frac{d\sigma_x}{dx} m = 0 \tag{9}$$

Based on the limit equilibrium condition and the Mohr Coulomb criterion, we have

$$2C_m + 2\sigma_z \tan\varphi - \frac{m(1 - \sin\varphi)}{1 + \sin\varphi}\frac{d\sigma_z}{dx} = 0 \tag{10}$$

Fig. 5 Schematic of plastic failure zone in the floor

Fig. 6 Stress analysis under equilibrium state

Knowing that under the distance $x = 0$, the horizontal stress $\sigma_x = 0$. Substituting this boundary condition into Eq. (10), the vertical stress is derived as

$$\sigma_z = \frac{1 + \sin\varphi}{1 - \sin\varphi} C_m \cot\varphi\, e^{\frac{2(1+\sin\varphi)x\tan\varphi}{m(1-\sin\varphi)}} - C_m \cot\varphi \qquad (11)$$

The plastic zone width is, therefore, calculated under the maximum abutment pressure condition $\sigma_z = k\gamma h$:

$$x_a = \frac{m(1 - \sin\varphi)}{2\tan\varphi(1 + \sin\varphi)} \ln \frac{(1 - \sin\varphi)(k\gamma H + C_m \cot\varphi)}{(1 + \sin\varphi)C_m \cot\varphi} \qquad (12)$$

where k is the peak concentration coefficient, γ represents the unit weight of the stratum, H is the average buried depth of the coal seam, φ is the internal friction angle of the coal seam, C_m represents the cohesion of the coal stratum, and m is the equivalent thickness of the excavation.
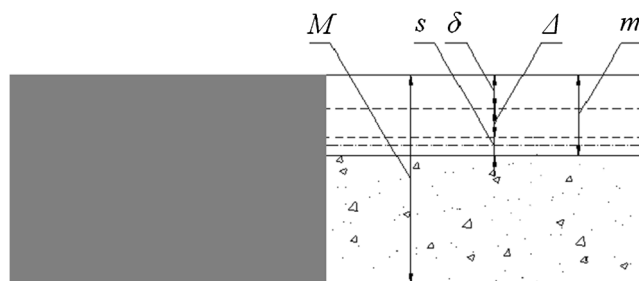
Calculation of the equivalent mining height

Figure 7 illustrates that the equivalent height (m) of the CPB working face consists of three parts, and can be calculated as.

$$m = \delta + \Delta + s(M - \delta - \Delta) \qquad (13)$$

where δ is the roof deformation, Δ is the gap between the roof and the CPB, M represents the average coal seam thickness, and s represents the CPB compression percentage.

Based on the geological condition of 2353 CPB working face, the coefficients s, δ, and Δ are 3%, 120–220 mm, and 0, respectively. The calculated equivalent mining height is around 200–300 mm. In addition, the coal seam cohesion

C_m is 0.5 MPa, the internal friction angle φ is 25°, and the peak concentration coefficient k is 4. The average unit weight of the stratum is 2500 kN/m^3. The friction angle of the bottom rock φ_0 is 35°. The calculated depth of the damaged floor is 2.5–3.0 m.

Field measurement of the damaged floor depth with CPB

For quantitatively observed damaged depth, the water injection into the floor through a drilling hole is used. This method is easy to use with relative low cost. To measure the excavation disturbance depth of the floor, a series of boreholes with different depth are drilled. The floor damage depth can be reflected by the water injection volume (WIV). The higher volume of the injected water, the more developed of the fracture.

Water injection borehole drilling scheme

For this observation, two (1# and 2#) observation stations are arranged in the belt haulage roadway and located at 70 m ahead of the mining terminal line. The distance between these two stations is 15 m. Each observation station consists of four boreholes (A1, A2, A3, and A4 and B1, B2, B3, and B4) with a spacing of 2 m (see Fig. 8). The drilling depth of the boreholes A1, A2, A3, and A4 in 1# station are 2 m, 3 m, 5 m, and 7 m, respectively, while the depth for the boreholes B1, B2, B3, and B4 in 2# station are 2 m, 4 m, 6 m, and 8 m, respectively.

Fig. 7 Equivalent mining height model
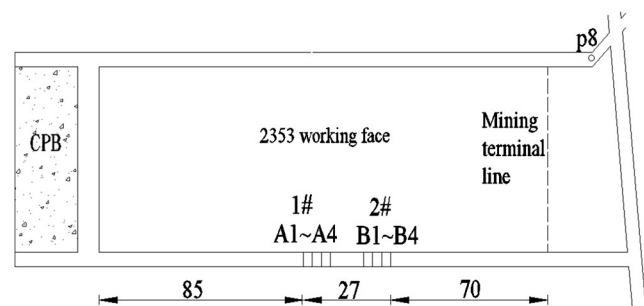
Fig. 8 Borehole drilling scheme

Fig. 9 Field measurement

Figure 9 illustrates the field measurement of one of the water injection boreholes. The water injection pressure was set as 0.15–0.2 MPa, and the water injection time keeps 15–25 min. The WIV data was recorded every 5 min.

Damaged floor depth analysis

Up to December 19th, 2016, a total of 5 effective data set were obtained. As of the last measurement, the working surface had been passed 15 m away from the last observation borehole of the 2# observation station. The water injection measurement data is shown in Table 2. It is worth to mention that the distance between borehole A1 and the CPB working face for the date August 8th, September 4th, October 18th, October 31st, and December 19th were 70 m, 54 m, 15.5 m, $-$0.5 m, and $-$43 m, respectively. The distance between the working face and other boreholes can be dynamically obtained based on the geometrical relationship among these boreholes.

It can be seen from Table 2 that the WIV increases as the working face advances in both observation stations. This tendency also coincides with the above

analyzed in the "Maximum floor damage depth" section that the damage depth increases when the distance between the working face and the measurement position decreases. For borehole A2 in 1# station, the sharp increment of WIV was observed on October 18th, and October 31st, which indicated that the fracture has propagated to the depth of 3 m below the coal seam floor. Under these observation dates (October 18th, and October 31st), the working face was 13.5 m behind and 2.5 m ahead of the A2 borehole, respectively. And the wivs of other boreholes in station 1 are the purpose of "almost no increase during the period" is to indicate that the floor crack of No. 1 station has expanded to 3 m below the floor of coal seam. The WIV fluctuated greatly in borehole B2 with the working face advances. The depth of borehole B2 was 4 m. Notably the WIV for boreholes A2 and B2 underwent a process of steady state, sharp increment, and gradually decrease state. This is because that the fracture width of the floor strata increased to the maximum value under tension condition, while it decreased under the compression stress when the working face reached the boreholes. An obvious increasement of the WIV was observed in B1, which was 33 m behind the working face on observation date October 31st. It can be concluded that the damaged depth of the station 2# is in a range of 2~4 m.

Based on the regulation regarding the reserved coal resource (under the building, aquifer, railway, and main coal pillars) excavation in China, the depth of the damaged floor with the traditional mining method is calculated as

$$h = 0.0085H + 0.1079L_x + 0.1665\alpha - 4.3579 \qquad (14)$$

By substituting the parameters of the 2353 working face, the depth of the damaged floor with traditional mining method reaches 16.15 m, while this value reduced significantly to around 3 m by using CPB mining method, resulting in 0.2

Table 2 Water injection data

Station	Borehole no.	Drilling depth/m	WIV/L min^{-1}				
			August 8th	September 4th	October 18th	October 31st	December 19th
1#	A1	2	0.39	0.19	0.1	0.06	–
	A2	3	0.28	0.11	7.04	5.02	–
	A3	5	1.09	1.08	1.00	1.13	–
	A4	7	0.26	0.34	0.41	1.60	–
2#	B1	2	0.02	0.07	0.12	5.14	–
	B2	4	0.05	0.12	2.04	1.26	0
	B3	6	0.09	0.68	0.30	0.10	–
	B4	8	1.93	1.13	2.16	0.94	0

times of the original. The backfilled CPB controls well with the rock deformation.

Conclusions

This paper addressed the confined pressure issue during the 2353 working face, Daizhuang Coal Mine excavation by using CPB mining method. The coal seam excavation with CPB mining method is equivalent to reducing the original mining thickness. The numerical simulation based on the Midas/GTS-Flac^{3d} technique is performed to study the failure characteristic of the coal seam floor. The depth of the coal seam floor by using CPB mining method is predicted through the slip line field theory of plastic mechanics. The main findings are summarized as follows:

(1) The simulation results indicate that the floor deformation is well controlled by using CPB mining method. Notably the tensile zone reduces greatly to one-sixth of the size with traditional caving mining method.

(2) The CPB mining method is considered lowering excavation thickness of the coal seam. The depth of the damaged floor is calculated as $2.5 \sim 3.0$ m based on the slip line field theory. The disturbed zone is further divided into three zones, namely active limit zone, transition zone, and passive limit zone. The maximum depth appears in the transition zone.

(3) The in situ observation results indicate that the depth of the fracture floor is around $2 \sim 4$ m. The numerical and analytical predictions in terms of floor damage depth have a good agreement with in situ measurement. The proposed analytic model provides insight into the floor behavior with backfilling mining method.

References

Chen W-F, ed. (2013) Limit analysis and soil plasticity. Elsevier

Dong X, Karrech A, Basarir H, Elchalakani M, Qi C (2018a) Analytical solution of energy redistribution in rectangular openings upon in-situ rock mass alteration. Int J Rock Mech Min Sci 106:74–83

Dong X, Karrech A, Basarir H, Elchalakani M (2018b) Extended finite element modelling of fracture propagation during in-situ rock mass alteration. In 52nd US Rock Mechanics/Geomechanics Symposium. American Rock Mechanics Association

Dong X, Karrech A, Basarir H, Elchalakani M, Seibi A (2019a) Energy dissipation and storage in underground mining operations. Rock Mech Rock Eng 52(1):229–245

Dong X, Karrech A, Qi C, Elchalakani M, Basarir H (2019b) Analytical solution for stress distribution around deep lined pressure tunnels under the water table. Int J Rock Mech Min Sci 123:104124

Duoxi Y, Lu H (2010) Coupling analysis of damage regularity of coal seam floor during mining above confined aquifer. Journal of Anhui University of Science and Technology (Natural Science) 30(4):5–10

Fengda Z, Baohong S, Yonghua K (2016) Water inrush failure mechanism of mining floor under unloading effect. Rock Soil Mech 37(2): 431–438

Guo GL, Zhu XJ, Zha JF, Wang Q (2014 Oct 1) Subsidence prediction method based on equivalent mining height theory for solid backfilling mining. Trans Nonferrous Met Soc China 24(10): 3302–3308

Hongfei D, Zhenquan J, Zhu S (2011) Measurement of mining-induced floor failure regularity for thin coal seams using fully mechanized coal caving. Journal of Mining & Safety Engineering 28(3):407–414

Jian S, Wang L, Furong T (2011) Microseismic monitoring failure characteristics of inclined coal seam floor. Rock Soil Mech 32(5):1589–1595

Lai X, Cai M, Ren F, Xie M, Esaki T (2006) Assessment of rock mass characteristics and the excavation disturbed zone in the Lingxin coal mine beneath the Xitian river, China. Int J Rock Mech Min Sci 43(4):572–581

Lu Y, Wang L (2015) Numerical simulation of mining-induced fracture evolution and water flow in coal seam floor above a confined aquifer. Comput Geotech 67:157–171

Qingliang C, Weijun T, Xiushan L (2016) Study on field measurement and floor failure law of paste filling fully mechanized mining. Journal of Mining & Safety Engineering 33(1):96–101

Qinglong S, Xu D, Mei Q (2013) Improved on the formula about the depth of damaged floor in working area. J China Coal Soc 38(s2): 299–303

Rui Z, Zhenquan J, Zuncai Y (2012) In-situ dynamic observation and numerical analysis of thick coal seam floor's failure law under the mining. Journal of Mining & Safety Engineering 29(5):625–630

Songping Z, Wu J, Shengdong L (2006) Study on dynamic observation of coal seam floor's failure law. Chin J Rock Mech Eng 25(s1):3009–3013

State Administration of work safety. Accident inquiry system [OL]. [2017-1-10]

Wang J-A, Park HD (2003) Coal mining above a confined aquifer. Int J Rock Mech Min Sci 40(4):537–551

Wang L, Meng H, Zhansheng W (2013) Stress distribution and damage law of mining floor[J]. Journal of Mining & Safety Engineering 30(3):317–322

Weidong L, Yang Y, Ma J (2015) Study on geo- stress measurement and distribution features in Jibei mining area. Coal Science and Technology 43(11):32–37

Wenquan Z, Kai Z, Guibin Z (2015) Prediction of floor failure depth based on grey correlation analysis theory. J China Coal Soc 40(s1):53–59

Xiucai Q, Gao M, Cheng Z (2016) Research floor damage mechanism on mining above confined water. Safety in Coal 47(1):51–54

Yaodong J, Yukai L, Yixin Z (2011) Similar simulation test for breakage law of working face floor in coal mining above aquifer. Chin J Rock Mech Eng 30(8):1571–1578

Yin WZ, Li D, Luo XM, Yao J, Sun QY (2016) Effect and mechanism of siderite on reverse flotation of hematite. Int J Miner Metall Mater 23(4):373

Yu X, Jin H, Qinglong S (2009) Forecast of destroyed floor depth based on BP neural networks. J China Coal Soc 6:731–736

Zhang J (2005) Investigations of water inrushes from aquifers under coal seams. Int J Rock Mech Min Sci 42(3):350–360

Zhang Y, Huang P (2019) Influence of mine shallow roadway on airflow temperature. Arab J Geosci 13. https://doi.org/10.1007/s12517-019-4934-7

Zhang J, TianQuan L (1990) On depth of fissured zone in seam floor resulted from coal extraction and its distribution characteristics. Journal of China Coal Society 15(2)

Zhang B, Xu D, Liu Y, Li F, Cai J, Du L (2016) Multi-scale evapotranspiration of summer maize and the controlling meteorological factors in North China. Agric For Meteorol 216:1–12

Zhu WC, Wei CH (2011) Numerical simulation on mining-induced water inrushes related to geologic structures using a damage-based hydro-mechanical model. Environ Earth Sci 62(1):43–54